J. Fluid Mech. (1975), *vol.* 71, *part* 1, *pp.* 123–144
Printed in Great Britain

Optical compensation measurements on the unsteady exit condition at a nozzle discharge edge

By D. BECHERT AND E. PFIZENMAIER
DFVLR-Institut für Turbulenzforschung, 1 Berlin 12, Müller-Breslau-Strasse 8

(Received 22 July 1974)

The exit condition at the trailing edge of a nozzle for slightly unsteady flow has been investigated experimentally. This problem plays a crucial role in sound transmission through nozzles with flow. The measuring technique used is new and is based on the synchronization of a laser beam to the wave motion of a small smoke filament in the boundary layer leaving the nozzle. The resolution of the jet flow deflexion measurements is of the order of 1–3 μm. The authors found the jet deflexion envelope to have a nearly parabolic shape near the nozzle edge. The size of this 'parabolic' region decreases with decreasing Strouhal number. This statement applies to the motion of the exterior border of the boundary layer at the dividing streamline between flow originating from the interior of the nozzle and flow coming from outside. It was found that the unsteady flow problem near the edge remains linear for fluctuating velocities of small magnitude.

1. Introduction

Experiments have been carried out on the exit condition at a nozzle discharge edge for a weakly unsteady jet flow. This investigation is closely connected with the problem of sound transmission through a nozzle with flow. Because of the increased bypass ratios of modern aircraft engines, the pure jet noise (see Lighthill 1952, 1954) has been reduced, with the result that compressor noise, engine thrust fluctuations and internal engine tones often dominate the noise radiated by the engine. Sound from these sources is transmitted through the nozzle and interacts with the jet flow on its way into the atmosphere.

The wavelike motion of jet flows has been studied since the beginnings of stability theory in the last century. In all the early investigations the jet flow was assumed to be parallel and of infinite extent in the streamwise direction. The problem has been solved for compressible flows too, and it is a well-known fact that the fluctuating pressure field decays rapidly in the direction perpendicular to the surface of the free shear layer. For perturbations with subsonic phase velocities in a plane flow problem, the fluctuating pressure decays exponentially with increasing distance. In the case of a circular jet, the fluctuations decay even faster, namely like a modified Bessel function. So we are left with the fact that for subsonic wave motions of parallel and infinitely long jets no sound is radiated.

This situation changes if the phase velocity and/or amplification rate of the instability waves of the jet are changed by spreading of the jet or by nonlinearities

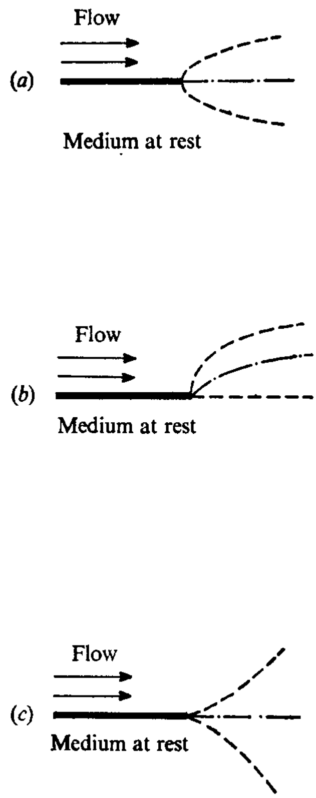

FIGURE 1. Trailing-edge conditions for a semi-infinite plate according to Orszag & Crow. (a) Envelope is a parabola (not a Kutta condition). (b) 'Rectified' Kutta condition. (c) 'Full' Kutta condition. – – –, envelope of the boundary-layer motion; —·—, jet boundary (steady part of the flow).

in the flow. Nevertheless it is sufficient to take into account the changing boundary conditions at the nozzle exit to obtain strong sound radiation from the wave motion of the jet flow. This latter fact was pointed out by Crighton (1972a, b) and the experimental study of these boundary conditions is the aim of this paper.

The first to consider the interaction between the instability waves in a free shear layer and the surface from which the shear layer is shed were Orszag & Crow (1970). They achieved an analytical solution for the case of an infinitely thin shear layer shed from a semi-infinite plate. The theory was expanded by Crighton (1972a, b), who took compressibility into account. In Orszag & Crow's (1970) investigation three possible conditions at the trailing edge of the plate were considered (see figure 1). They evaluated the solutions of all three cases, but could not give conclusive support for any one of these possibilities.

Bechert & Pfizenmaier (1971) carried out some experiments which showed that condition 2 (the 'rectified Kutta condition') does not apply at low magnitudes of the fluctuating flow. This is the region where linearized theories can be applied, and it was shown by their experiments that no velocity singularity occurs at the trailing edge of the nozzle. This statement is amplified by the present investigation (see also Bechert & Pfizenmaier 1973). Moreover, a 'rectification' effect would imply that the non-equilibrium of the steady static pressure on either side of the deflected boundary layer should be balanced by nonlinear effects in the equations of motion. This can take place only for velocity fluctuations of sufficiently high magnitude. Since we exclude velocity fluctuations of high magnitude, the 'rectified Kutta condition' can be rejected.

Two investigations have been published on the interaction of a pulsating source and a free shear layer shed from a semi-infinite plate. Crighton & Leppington (1974) considered this problem with the introduction of compressibility effects. In their paper acoustical radiation properties are discussed in some detail; and it is shown that sound radiation and hydrodynamical instability of the semi-infinite shear layer are coupled. For the behaviour of the flow at the trailing edge they found that there are an infinite number of causal solutions for the boundary-layer motion excited by the pulsating source, just one of which satisfies the 'full Kutta condition'. They state that the proper choice of the exit condition is determined by the fluctuating flow in the vicinity of the edge, for which analytical solutions are not yet available.

Bechert & Michel (1974, 1975) considered the same problem with the restriction to an incompressible fluid. This additional simplification allowed the introduction of a simple mathematical technique based on the symmetry of pressure gradients on either side of the free shear layer. In addition, this symmetry consideration led to the rejection of that class of solutions which contains the 'parabolic condition', according to Orszag & Crow. So only the 'full Kutta condition' was found to be possible. Moreover, Bechert & Michel found that only forced motions of the semi-infinite shear layer can occur.

It can be shown that the symmetry considerations which lead to the rejection of the 'parabolic condition' break down for a compressible flow with finite Mach number. The reason is that the wave equations of the pressure fluctuations on either side of the shear layer become different. Consequently, the symmetry of the pressure gradients on either side of the shear layer is lost. However, for $M \to 0$ both the symmetry of the pressure field induced by the boundary-layer perturbations and the 'full Kutta condition' are recovered.

In all available theories the boundary-layer thickness is assumed to be zero. In practical applications we are confronted with a finite boundary-layer thickness at the nozzle discharge edge. If one considers the boundary-layer thickness θ to be an essential parameter and the Strouhal number S_θ (formed with the boundary-layer thickness) to be the corresponding dimensionless quantity of essential significance, one can extend these (more or less speculative) considerations by dimensional analysis (see, for example, Bechert 1971); one finds that at very low Strouhal numbers S_θ the flow in the vicinity of the edge should behave like a steady flow; i.e. the 'full Kutta condition' should apply. On the other hand at high Strouhal numbers S_θ the behaviour of the fluctuating flow should be similar to the case in which there is no mean flow. This means that at high Strouhal numbers S_θ no Kutta condition is to be expected. Thus we feel that our investigation is not very useful for determining the exit condition for an *infinitesimally* thin boundary layer. In contrast, the present experimental data may help to establish theories which take into account the finite thickness of the boundary layer.

However, one is interested in the following question: what is the best asymptotic description of the behaviour of the exterior potential flow around the jet? This is because this property yields information about the sound radiation of the flow. If we expect, as mentioned above, a transition from the 'full Kutta condition' to some sort of 'parabolic condition' with increasing Strouhal number, it is a reasonable approach to try a superposition of the contributions of both conditions as a preliminary model. Obviously this model is restricted to 'not too high' Strouhal numbers S_θ. Nevertheless, it does not seem to be sensible to try such a general semi-empirical description of the subject with the present state of the theory. If not even the axial symmetry were taken into account in the available theories, one would be restricted to relatively high Strouhal numbers S_D (formed with the diameter D of the nozzle) at which the axial symmetry plays no important role. On the other hand at high Strouhal numbers S_θ (based on the momentum thickness θ of the boundary layer) the boundary-layer thickness is a most important parameter and causes deviations from the behaviour of an infinitesimally thin shear layer. So, at present, the range of parameter variation would be too limited. Consequently, the present investigation was restricted to merely an experimental consideration of the effects in the vicinity of the trailing edge and their dependence on the Strouhal and Reynolds numbers.

We found that our previous measurements (Bechert & Pfizenmaier 1971) of the jet border deflexion were correct, but not accurate enough in magnitude and point resolution. Moreover, the restriction to one Strouhal number seemed to be too limiting to permit general statements.

In order to obtain more conclusive results, we expanded the present experiments to cover the whole frequency range of amplified waves in the boundary layer. In addition, we developed a new optical measuring technique to measure the deformations of the jet boundary layer. Hot-wire measurements were carried out to make sure that the interaction between the fluctuating and mean flow is a linear one.

2. Measuring technique

2.1. *The free jet test facility*

The free jet test facility (see figure 2) was nearly the same as that used in our previous experiments (Bechert & Pfizenmaier 1971). Since we used smoke injection in our optical measurements, we disconnected the closed air circuit of the former test facility in order to avoid increasing pollution by smoke in the test chamber. In addition, an infra-sound silencer was mounted on the pressure side of the radial fan to prevent infra-sound components, produced by the radial fan, from being transmitted to the test chamber. It consisted mainly of a porous plastic-foam tube. By means of this absorber the r.m.s. value of low frequency pressure fluctuations in the settling chamber could be reduced by about 10 db. Part of this effect was due to a complete vibration disconnexion between the

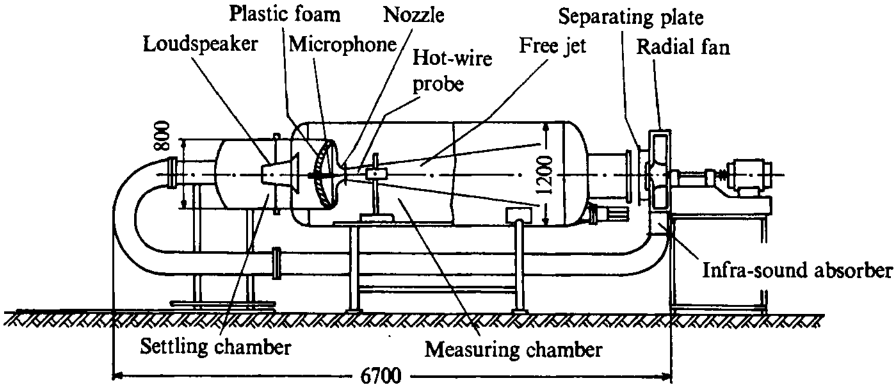

FIGURE 2. Free jet test facility. Dimensions in mm.

radial fan and test chamber. We suppressed disturbances of the nozzle boundary layer, which arose from flow separations within the settling chamber, by using a plastic-foam rectifier upstream in front of the nozzle (see figure 3). Air flowing downstream out of this plastic-foam rectifier was always accelerated, up to the nozzle exit plane.

A so-called vortex filament nozzle, whose wall shape is that of the streamlines of a potential ring vortex, was used. The contour and boundary layer of this type of nozzle were given by Michalke (1962). On the axis of a vortex filament nozzle a simple expression relates the fluctuating velocity and fluctuating pressure, as shown in Bechert & Pfizenmaier (1973). The measurements were carried out with nozzles of 30 and 100 mm diameter at the exit plane. The mouth of each nozzle was surrounded by an annular disk which had an exterior diameter three times that of the nozzle exit plane. Thus a nozzle lip contour nearly equivalent to a rectangular nozzle discharge edge was produced (see figure 3).

The jet flow disturbances starting from the nozzle discharge edge were controlled and synchronized by a loudspeaker in the settling chamber. Two different exchangeable loudspeaker systems of 20 and 38 W power were used. Both systems were installed as a closing diaphragm of a cylindrical cavity. The different frequency responses of both systems overlapped in such a way that maximum sound pressure levels of 110–130 db in the nozzle could be reached over a frequency range from 27 Hz to 1 kHz. The reference sound pressure level was measured at an axial position 1·5 diameters upstream of the nozzle exit plane using a condenser microphone with a nose cone. We used a $\frac{1}{4}$ in. microphone for the 30 mm diameter nozzle and a 1 in. microphone for the 100 mm diameter nozzle.

2.2. *Optical compensation measuring technique*

The wavelike deformation of the jet border by the sound field has been determined by a new optical measuring technique (see figure 4). A very thin smoke filament is blown tangentially to the nozzle surface into the nozzle boundary layer. The smoke filament leaves the nozzle with the free jet flow and follows the boundary-layer motion with no significant slip. (For more details see Bechert & Pfizenmaier 1973.)

The smoke filament is now illuminated by a light beam. The light beam is

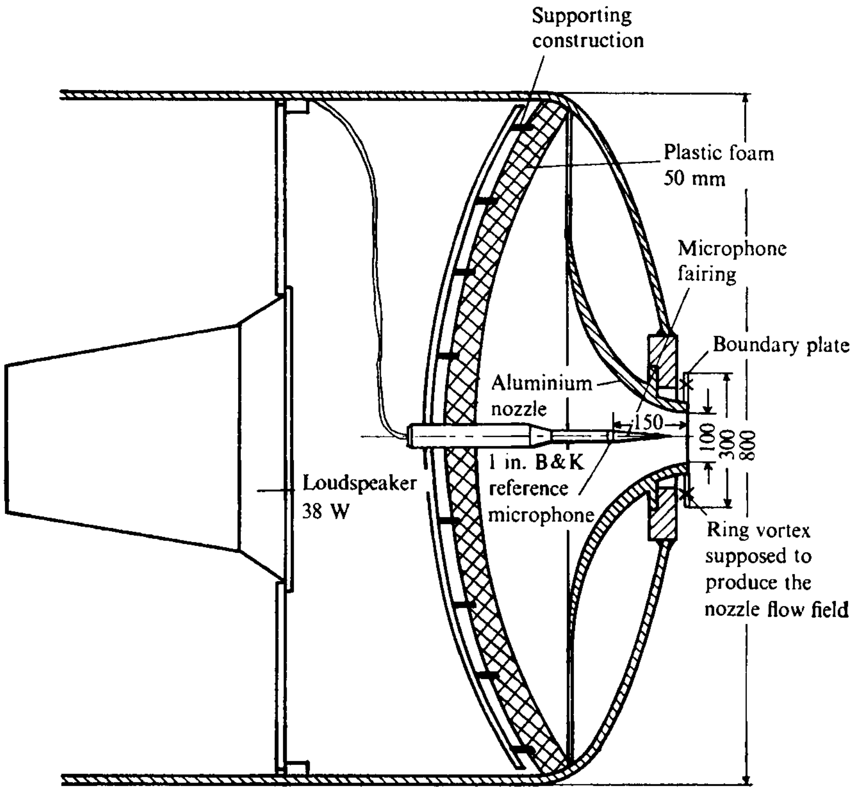

FIGURE 3. Settling chamber, vortex filament nozzle, loudspeaker and reference microphone. Dimensions in mm.

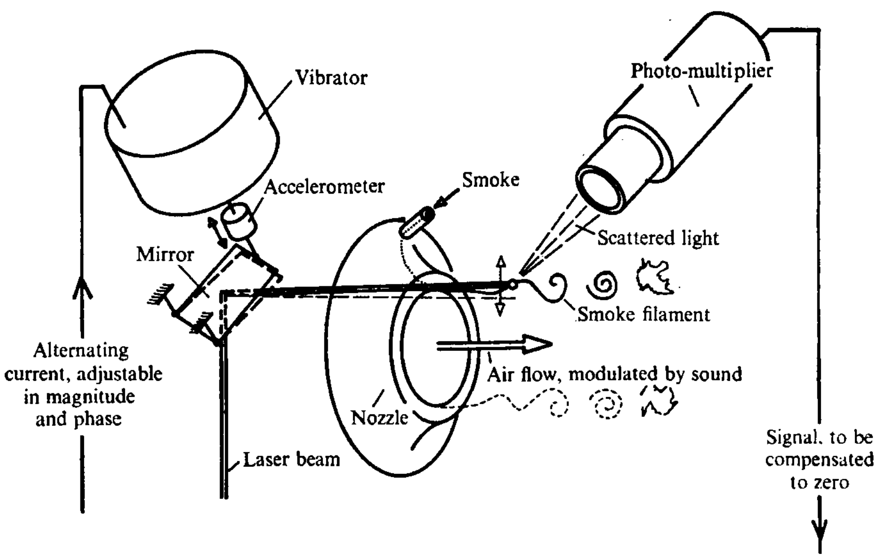

FIGURE 4. Principle of the optical compensation measuring technique.

directed perpendicular to the flow direction of the smoke filament and tangential to the surface of the circular jet. Where the light beam and the smoke filament cross a light dot is produced. If the smoke filament moves in a wavelike manner, the light dot suffers intensity fluctuations, which can be measured, e.g. by a photo-multiplier. If we also move the light beam by means of a vibrating mirror in such a way that it follows the smoke filament in magnitude and phase, then *no* intensity fluctuations of the light dot occur. After a calibration procedure, the motion of the mirror is then a quantitative measure of the deflexion of the jet boundary.

As a light source we used a helium–neon laser of 15 mW light power output. The mirror was shaken by a Bruel & Kjaer vibrator, type 4809. A Bruel & Kjaer accelerometer was used to determine the phase of the mirror's motion. The driving voltage of the vibrator had the same frequency as the sound field which influenced the nozzle flow. We could vary this voltage in amplitude and phase until constant intensity of the light dot was achieved. This was verified on the screen of an oscilloscope which was fed with the filtered signal of the photo-multiplier.

The optical measuring arrangement could be moved on a support parallel to the mean flow direction. Figure 5 (plate 1) shows a photograph of the cross-section of the smoke filament in the exit plane of the 100 mm diameter nozzle at

$$Re = 5 \times 10^4.$$

The grid in the lower part of the picture is the 1 mm square pattern of millimetre paper glued on the mouth of the nozzle. The inner surface of the nozzle is coated with a thin gold sheet to prevent corrosion of the nozzle by the smoke.

If we move the light beam slowly across the smoke filament we reach somewhere the border between smoke and clean air. This is the position of the largest smoke intensity gradient. At this location of the light beam, we obtain a maximum in the light-intensity fluctuations if the smoke filament vibrates and the position of the light beam remains fixed. Since the smoke filament has two borders, we have two maxima of the light-intensity fluctuations. We chose the exterior maximum for our measurements, which is more or less identical with the position of the bounding streamline of the free jet. We compensated this maximum to zero by adjusting the mirror vibration.

2.3. *Hot-wire technique*

The hot-wire measurements were carried out with a hot-wire anemometer of the constant-temperature type, with a linearization unit which approximated the hot-wire characteristics continuously. This hot-wire anemometer (HDA III) has been developed by Dipl.-Ing. E. Froebel at the DFVLR-Institut für Turbulenzforschung in Berlin.

We used probes with wires 2 mm long; the hot wire was adjusted perpendicular to the mean flow direction and tangential to the surface of the jet. This adjustment allowed measurements of the $\tilde{u}$ fluctuation component in the mean flow direction only. The probe could be moved in the radial direction either by a support driven by a synchronous electromotor or by a micrometer screw driven manually. The position of the probe could be verified by a microscope and the distance from the nozzle edge position could be read by extensometers.

3. Determination of significant ranges of parameter variation

In all experimental set-ups the variation of parameters is limited. Bounds for the parameter variation are both physical effects in the situation under consideration and restrictions caused by the measuring technique. We call this restricted parameter space the 'experimental window'. The determination of the frame of this window corresponds to the determination of the bounds of parameter variation. In the present paper, we shall restrict ourselves to a short discussion of the main parameter bounds; for more details see Bechert & Pfizenmaier (1973).

In principle, the physical problem of this investigation, the 'unsteady exit condition at a nozzle discharge edge', can be described by means of the five partial differential equations of the motion of gases. These are the continuity equation, the isentropy condition and the three equations of motion. One set of possible dimensionless parameters of this system consists of the Reynolds number, Mach number and Strouhal number. Bechert (1971) has shown in a more detailed investigation of this set of dimensionless parameters that compressibility effects can be neglected if both the Mach number and its product with the Strouhal number are small. This product we call here the Helmholtz number He. It represents the ratio between a typical length of the problem (e.g. the nozzle diameter D) and the wavelength of sound in the fluid at rest λ:

$$He = MS_D = \frac{U_0}{a_0}\frac{fD}{U_0} = \frac{fD}{a_0} = \frac{D}{\lambda}. \tag{1}$$

We restricted our measurements to the incompressible region $M \ll 1$, $He \ll 1$. Thus the problem depends on the Strouhal number and the Reynolds number only. No other dependence on a ratio of lengths exists for any combination of parameters using a nozzle of similar shape; e.g. the boundary-layer thickness of the free jet is related to the nozzle diameter by the Reynolds number. Therefore the ratio of the boundary-layer thickness and nozzle diameter does not create another independent variable in this system. If the Helmholtz number exceeds a certain value, the incompressibility simplification is no longer applicable. For a region within 1·5 nozzle diameters from the nozzle exit plane, incompressibility is sustained if the Helmholtz number does not exceed the value $He = 0{\cdot}08$. This boundary was determined experimentally (see Bechert & Pfizenmaier 1973) by comparing the calculated sound pressure distribution for the incompressible nozzle flow with the distributions measured at different Helmholtz numbers.

The bounds on the Helmholtz number are shown in a log–log plot of the Strouhal and Reynolds numbers (see figure 6). We obtain inclined straight lines with gradient -1 for the two different nozzle diameters which were used. In the region below each of these lines, compressibility can be neglected. The Strouhal number S_D in figure 6 is based on the nozzle diameter. Since it is not quite clear whether the Strouhal number S_θ (based on the boundary-layer thickness) is actually

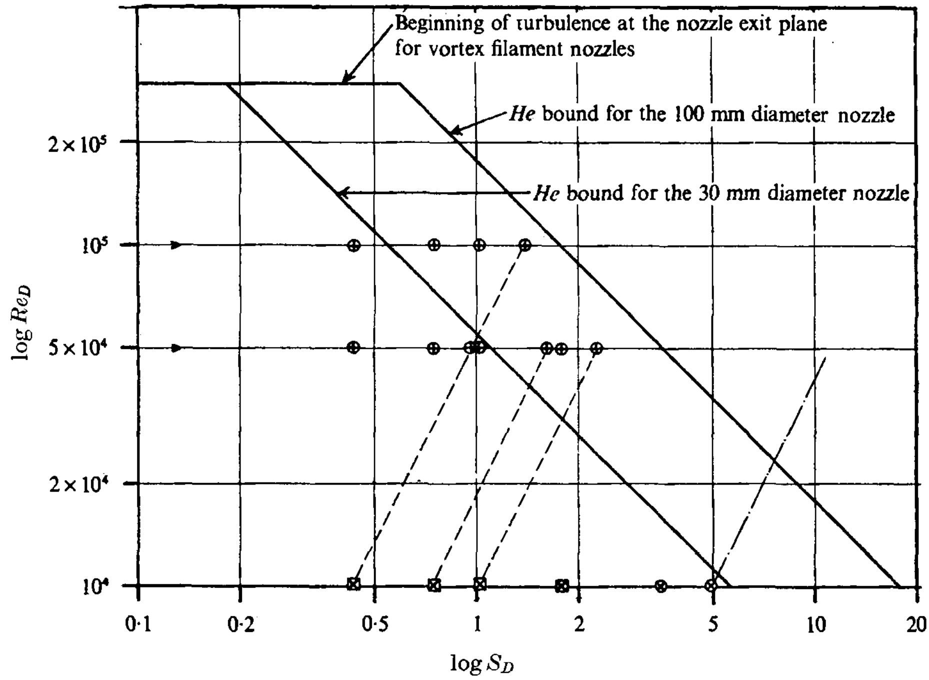

FIGURE 6. Measuring points and ranges of parameter variation. ---, constant Strouhal number $S_\theta = f\theta/\overline{U}_0$; —·—, neutral-stability curve for waves in free shear layer. Measuring points: ×, 30 mm nozzle, hot-wire data; □, 30 mm nozzle, optical compensation measurements; +, 100 mm nozzle, hot-wire data; ○, 100 mm nozzle, optical compensation measurements. $S_D = fD/\overline{V}_0$.

the more appropriate parameter, lines of constant S_θ are plotted in figure 6 too. A typical measure of the boundary-layer thickness is the momentum thickness θ_m (Freymuth 1966):

$$\theta_m = 0{\cdot}61 D/Re_D^{\frac{1}{2}}. \qquad (2)$$

S_θ is defined as

$$S_\theta = f\theta_m/\overline{U}_0, \qquad (3)$$

where f is the frequency of the sound and $\overline{U}_0$ is the mean velocity at the exit of the nozzle. Lines of constant S_θ have a gradient of $+2$ in figure 6. The neutral-stability curve of the jet waves (see figure 6) is almost entirely dependent on the Strouhal number S_θ for sufficiently low values of θ_m/D. This neutral-stability curve is also given in figure 6. The ratio θ_m/D was of the order of 0·01 in our experiments.

For very low Strouhal numbers the fluctuating pressure at the reference microphone is no longer independent of the mean flow velocity. At the lowest Strouhal number of our experiments, $S_D = 0{\cdot}435$, this effect is not yet detectable.

An upper bound for the Reynolds number is given by the fact that at values above $Re_D \approx 3 \times 10^5$ the transition from laminar to turbulent flow in the boundary layer of the vortex filament nozzle occurs just before it leaves the nozzle edge. In a turbulent boundary layer the optical compensation breaks down, because the smoke filament spreads very rapidly. Moreover the turbulent fluctuations would cause additional difficulties.

An essentially enlarged parameter variation could be achieved only by abandoning the incompressibility condition or by changing the fluid.

Practical sound pressure levels for this investigation were first selected for a Reynolds number $Re = 10^4$. Sound pressures of about 100 db turned out to exceed the natural excitation of the free shear layer at the nozzle exit plane by more than 20 db. Thus for the first series of measurements at $Re = 10^4$ sound pressure levels of 104, 94 and 84 db were chosen arbitrarily, the latter being nearly of the order of the natural excitation. These levels were kept constant at $Re = 10^4$ for all Strouhal numbers. For higher Reynolds numbers the same relation between the fluctuation amplitude and mean flow velocity was chosen. Therefore the sound pressure levels were changed at higher Reynolds numbers. This sound pressure level conversion was verified at $Re = 10^4$ and $S_D = 1{\cdot}77$ using two different nozzle diameters. The nozzle diameters in the experiments were $D = 30$ mm for $Re = 10^4$ and $D = 100$ mm for $Re = 5 \times 10^4$ and $Re = 10^5$.

4. Measured results

4.1. *Mean velocity profiles*

The mean velocity profile and its geometrical location were measured with a hot-wire probe. The hot wire was orientated perpendicular to the mean flow direction and tangential to the surface of the circular jet. In this way only the total velocity, which is essentially equal to the axial velocity component of the jet, was measured by the hot wire. The measurements were carried out for the three Reynolds numbers $Re = 10^4$, 5×10^4 and 10^5, and at those axial distances x from the nozzle exit at which the light compensation measurements were made.

An example of these measurements is given in figure 7, where y is in the radial direction of the circular jet; the nozzle edge is defined as the origin $y = 0$. In addition, the location of the smoke filament in the mean velocity profile is shown; it was identified by using a microscope. The jet deflexion measurements refer to the exterior border of the smoke filament (see figure 7).

4.2. *Fluctuation measurements*

In this subsection measurements of both the jet deflexion and $\tilde{u}$ velocity fluctuation are given. The latter measurements were carried out in order to verify that linearity holds in the flow region under consideration.

For the optical compensation measurements the maximum value of the smoke-filament deflexion $\hat{h}$ was normalized by a typical fluctuation amplitude ξ:

$$\xi = p_0/\bar{\rho}\omega^2 D. \tag{4}$$

Here p_0 is the r.m.s. value of the sound pressure measured by the reference microphone, $\bar{\rho}$ is the density of the fluid, ω is the circular frequency of the sound and D is the nozzle diameter. The particle deflexion amplitude for a medium at rest at the location of the reference microphone is proportional to ξ and can be calculated if $He \leqslant 0{\cdot}08$ (see also Bechert & Pfizenmaier 1973). We define the normalized smoke-filament deflexion h^* as the ratio $\hat{h}/\xi$. By this normalization we obtain a single curve for different sound pressures. In addition, we can change the dia-

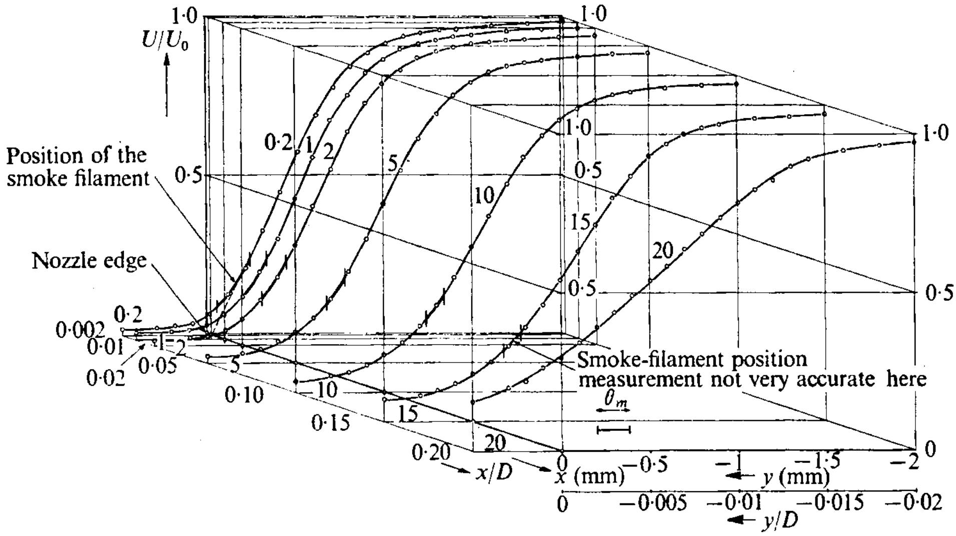

FIGURE 7. Development of the mean velocity profiles $\bar{U}(y)/\bar{V}_0 = f(x/D)$ downstream and position of the smoke filament for $Re = 10^5$ and $D = 100$ mm.

meter of the nozzle, which has some advantages for the experimental technique. We proved also for this latter case that one normalized h^* curve occurred if both the parameters Re_D and S_D were kept constant.

Figure 8 shows on the left-hand side an h^* curve for the parameter combination $Re_D = 10^5$, $S_D = 1{\cdot}373$. Below this curve the phase angle of the deflexion h^* is given with reference to the phase angle of the pressure at the reference microphone. The measurements of the dimensionless deflexion h^* for the two different sound pressures under consideration fall on one curve. This is one method of checking the linear behaviour of the flow field. Another investigation of how far the linear flow region extends can be performed by measuring the $\tilde{u}$ fluctuations in the shear layer. Measurements of this type are given on the right-hand side of figure 8. We assume that the behaviour of the maximum (in the radial direction) of the $\tilde{u}$ fluctuations in the free shear layer is suitable for a rough diagnosis of the beginning of nonlinearities in the flow field. Measurements of the maximum $\tilde{u}$ fluctuations are shown in the right-hand part of figure 8.

The upper diagram on the right-hand side shows a semi-logarithmic plot of the maximum of the $\tilde{u}$ fluctuation at two different reference sound pressures. The fluctuation velocity $\tilde{u}$ is normalized by the mean velocity $\bar{U}_0$ in the nozzle exit plane at the jet axis. These measurements were filtered at the frequency of the exciting sound field. The middle diagram gives the location of the maximum $\tilde{u}$ velocity fluctuation. The radial distance y is measured from the nozzle edge and is normalized by the momentum thickness θ_m [see (2)]. The lower diagram on the right-hand side gives the phase of the $\tilde{u}$ fluctuations with reference to the phase angle of the sound pressure at the reference microphone. The region of 'upstream-travelling waves' for $x/D < 0{\cdot}1$ in figure 8 is interpreted as resulting from the influence of the nozzle edge. The size of this region decreases with increasing Strouhal number (see also Bechert & Pfizenmaier 1973). Quantitative

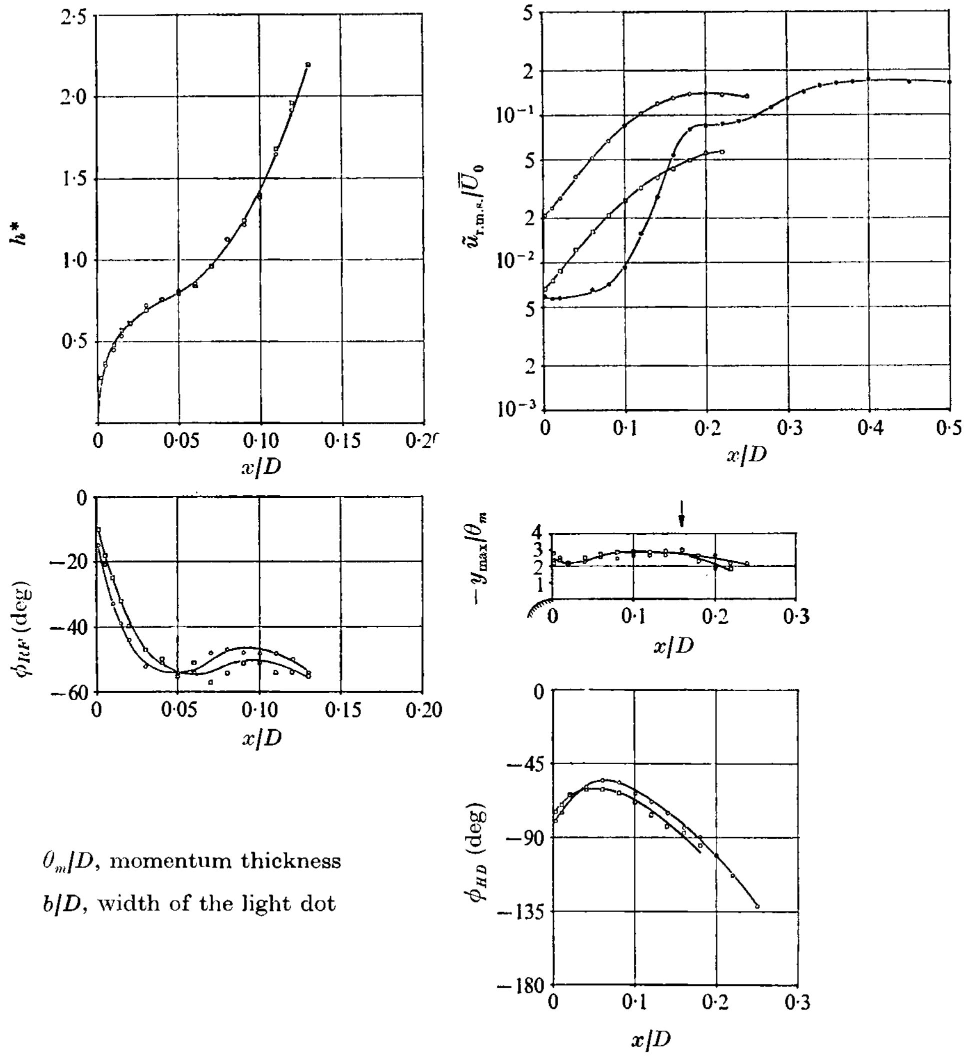

FIGURE 8. Fluctuation measurements: amplitude and phase. Left-hand side: optical compensation measurements. Right-hand side: hot-wire measurements. $Re = 10^5$, $S_D = 1{\cdot}373$, $S_\theta = 0{\cdot}00265$. ●, natural excitation; ○, 118 db; □, 108 db.

calculations based on the configuration of a shear layer shed from a semi-infinite plate with both the 'full Kutta condition' and the 'parabolic condition' show similar results. W. Möhring (Max-Planck-Institut für Strömungsforschung, Göttingen, private communication)† has contributed the calculation of the $\tilde{u}$ distributions at both the inner and outer edge of the shear layer. It turns out that the influence of the edge vanishes in $x \leqslant \bar{U}_0/\omega$.

† The $\tilde{u}$ distributions for $x > 0$ are the same as those calculated from the Kelvin–Helmholtz solutions for the $\tilde{v}$ distributions obtained asymptotically if the correction functions, which incorporate the influence of the semi-infinite plate, have vanished. The $\tilde{v}$ distribution can be determined from the deflexion distribution η (corresponding to h in our nomenclature) of Orszag & Crow (1970).

To give some additional background information, the natural disturbances of the uninfluenced free jets are given too. These measurements were not filtered. The amplification rate of the natural fluctuations changes rapidly in the downstream direction. The region nearest the exit of the nozzle is governed by low frequency perturbations of small amplification only. At a certain distance (in our example $x/D \approx 0{\cdot}1$) the boundary layer has filtered out those frequency components which are amplified rapidly. The fluctuations in this region are in a frequency band near the calculated frequency of maximum growth rate. Further downstream, saturation and the transition to turbulence take place (for more details see Miksad 1972).

We shall now return to the forced $\tilde{u}$ fluctuations in the shear layer. From theoretical calculations (see, for example, Michalke 1965, 1971) we expect exponential growth of the fluctuations in the free shear layer. This behaviour has been verified over a wide range of Strouhal numbers by Freymuth (1966). Nevertheless, some deviations from this behaviour should be mentioned: at very low Strouhal numbers the influence of the nozzle wall is dominant in the region of laminar flow downstream of the nozzle edge; on the other hand it has been shown by Pfizenmaier (1973) that at high Strouhal numbers, in the vicinity of the Strouhal number of neutral stability, some sort of standing wave pattern occurs. This pattern can be interpreted roughly to be the superposition of the forcing sound field and the field of the stability waves. It should be mentioned that this separation into two components is admissible at sufficiently high Strouhal numbers only (see, for example, Bechert 1971).

4.3. *Criteria for the nonlinear behaviour of the flow field*

Nonlinearities in the $\tilde{u}$ fluctuations clearly begin before saturation is reached. The simplest method of finding a nonlinearity effect is to look at the vertical separation of the two nearly parallel curves in the upper diagram on the right-hand side of figure 8. The measurements were taken at sound pressure levels differing by 10 db. Consequently, the curves should be shifted by the amount 3·16. At some distance downstream (here $x/D \approx 0{\cdot}15$) the distance between the curves decreases and nonlinearity of the upper curve begins to occur. In the same downstream region of incipient nonlinearity, the curves of the radial location $y_{\max}$ of the maximum $\tilde{u}$ fluctuation at the different sound pressure levels begin to separate. Looking at these criteria we ensured that the whole region downstream, following the nozzle edge, which we investigated by optical deflexion measurements of the smoke filament was essentially free from hydrodynamical nonlinearities.

4.4. *Comparison of measured results: the jet border deflexion h^**

A summary of the measured results is given in figures 9–11, where the deflexion h^* of the jet border is plotted as a function of the distance x/D downstream. In each of these diagrams the Reynolds number Re_D is kept constant and the Strouhal number S_D is varied.

For $Re_D = 10^4$ our measurements cover the whole range of Strouhal numbers in

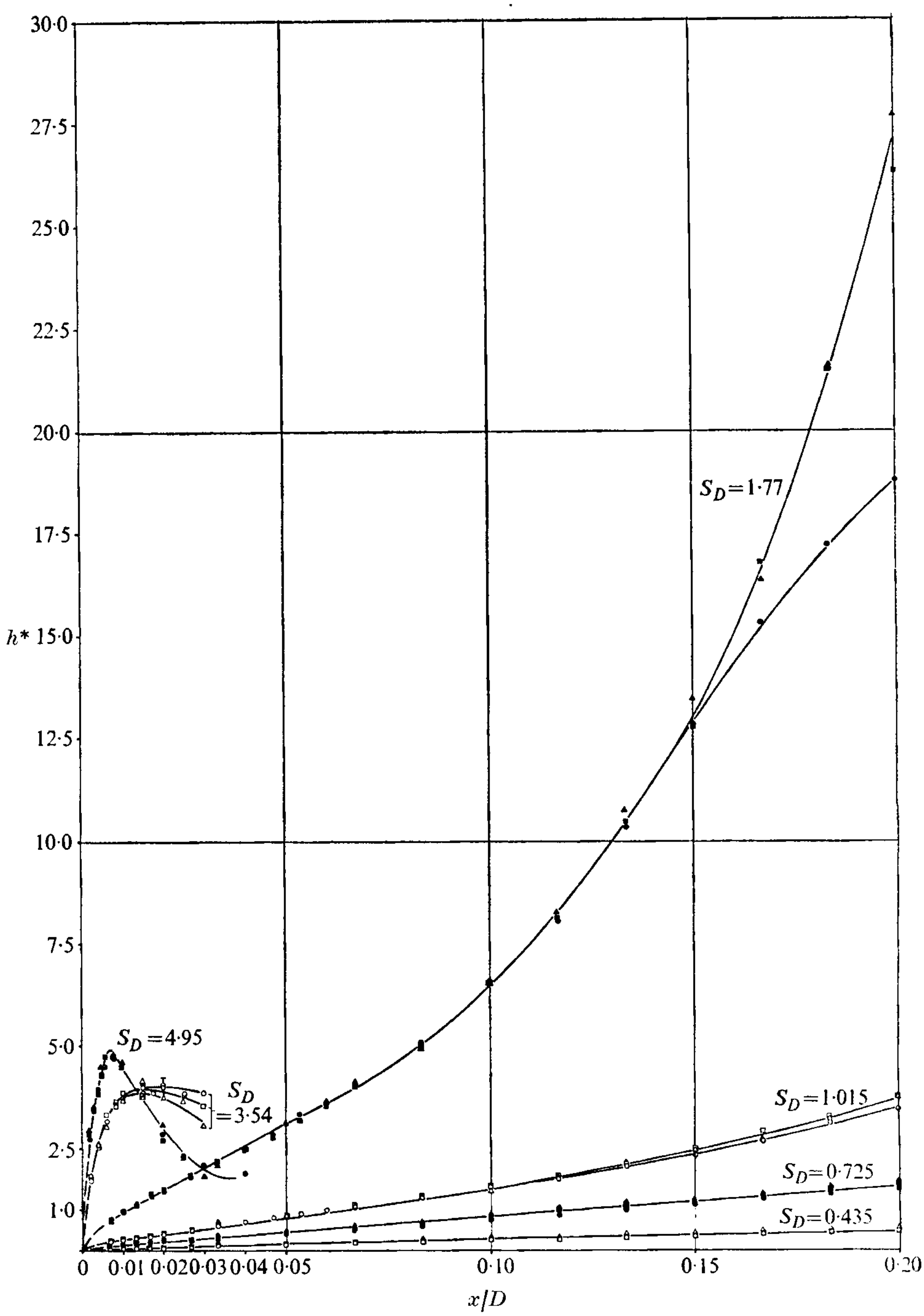

FIGURE 9. Optical compensation measurements: envelope of the jet border deflexion downstream. $Re = 10^4$, S_D varied. ○, ●, 104 db; □, ■, 94 db; △, ▲, 84 db.

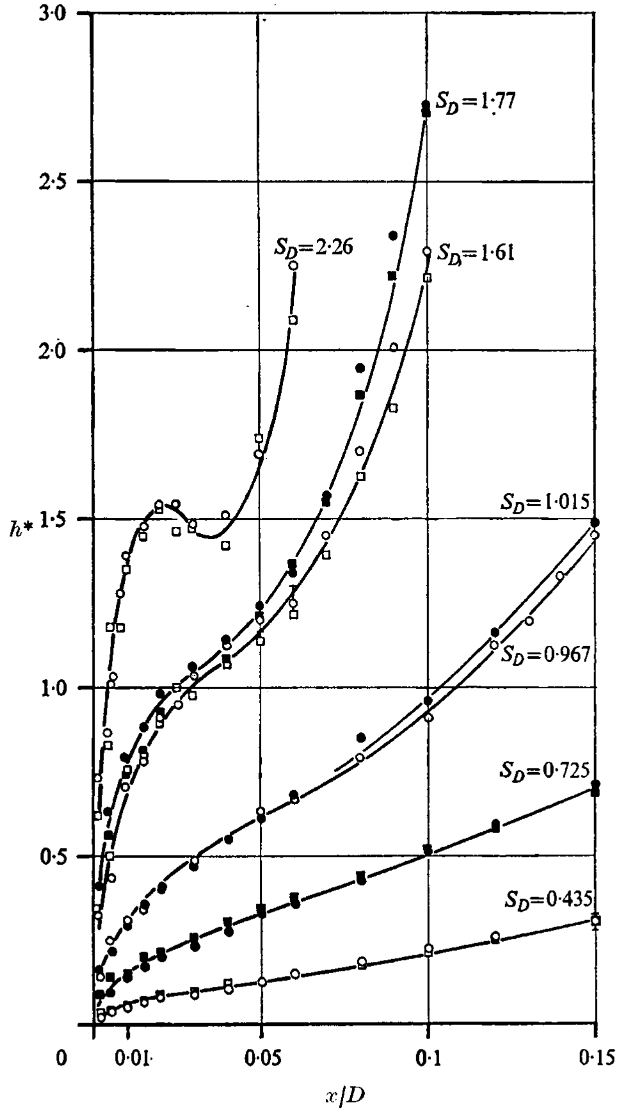

FIGURE 10. Optical compensation measurements: envelope of the jet border deflexion downstream. $Re = 5 \times 10^4$, S_D varied. ○, ●, 108 db; □, ■, 98 db.

which disturbances in the free shear layer are amplified (see also Freymuth 1966; Michalke 1971; Pfizenmaier 1973). At low Strouhal numbers, the jet border deflexion h^* resembles a straight line (even if the vertical scaling is enlarged). Near the trailing edge of the nozzle only a small region of parabolic shape can be detected. At $S_D = 1{\cdot}77$ the maximum amplification (for $Re_D = 10^4$) is reached Here h^* shows, after a significant parabola-like beginning, a very steep exponential growth. The curve splits at high x/D into different branches caused by hydrodynamical nonlinearities occurring at high sound pressure levels. For increasing Strouhal numbers the h^* curves become steeper at the nozzle edge. After a short

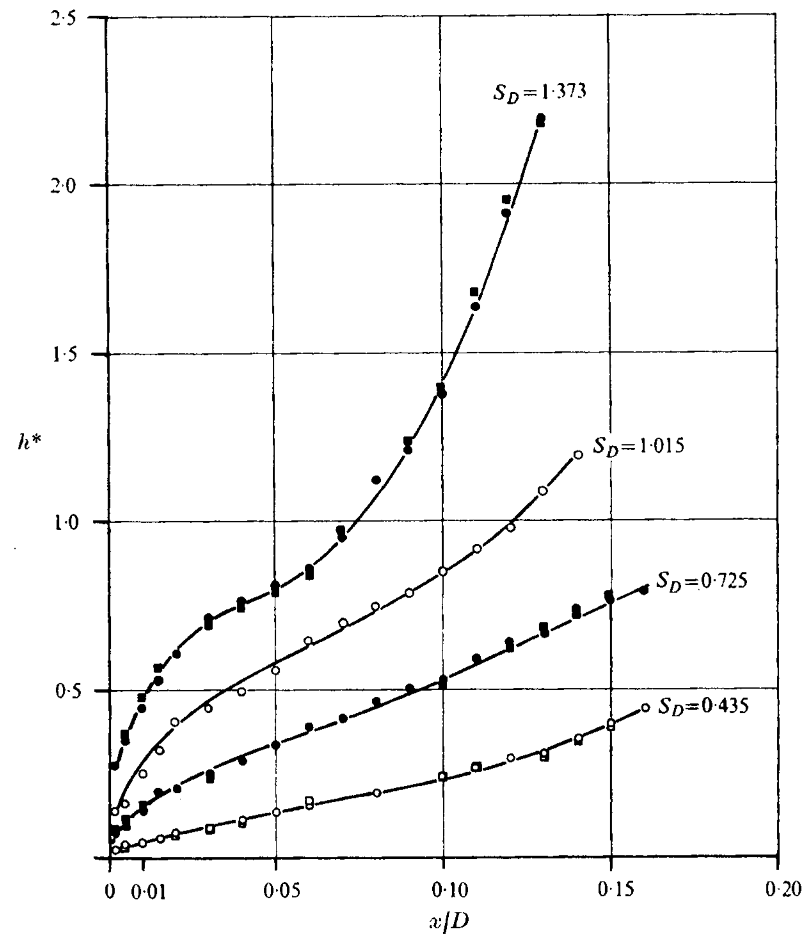

FIGURE 11. Optical compensation measurements: envelope of the jet border deflexion downstream. $Re = 10^5$, S_D varied. ○, ●, 118 db; □, ■, 108 db.

distance downstream the h^* amplitude decreases and no exponential growth follows (see figure 9, $S_D = 3{\cdot}54$ and $4{\cdot}95$). The jet border then shows more and more the behaviour of a fluctuation field around a nozzle edge without a superimposed flow field. This was expected from dimensional analysis for high Strouhal numbers (see, for example, Bechert 1971).

Measurements at higher Reynolds numbers (see figures 10 and 11) show, in principle, a similar behaviour. Nevertheless, it seems that the parabola-like development near the nozzle edge is already present at smaller Strouhal numbers. In connexion with this observation it should be mentioned that for the higher Reynolds numbers $Re_D = 5 \times 10^4$ and $Re = 10^5$ the bigger nozzle (diameter 100 mm) was used for the experiments. Therefore the size of the measuring point (diameter 0·23 mm) covers a smaller fraction of the parabola-like region near the nozzle edge. Consequently the measurement accuracy is better there.

Another summarizing representation is given in figures 12–14. The jet border

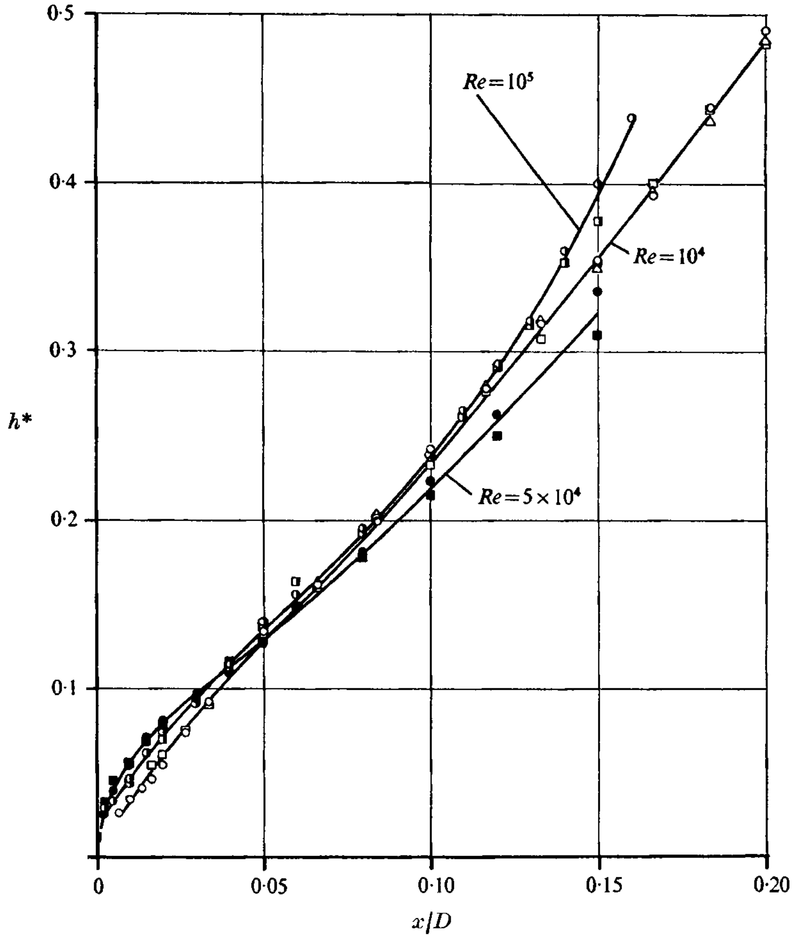

FIGURE 12. Optical compensation measurements: envelope of the jet border deflexion downstream. $S_D = 0{\cdot}435$. $Re = 10^4$: ○, 104 db; □, 94 db; △, 84 db. $Re = 5 \times 10^4$: ●, 108 db; ■, 98 db. $Re = 10^5$: ◑, 118 db; ◨, 108 db.

deflexion h^* is plotted again as a function of the distance x/D downstream. Now the Strouhal number S_D is kept constant in each diagram and the Reynolds number Re_D is varied. For the lowest Strouhal number, $S_D = 0{\cdot}435$ in figure 12, we notice a great similarity between the h^* curves. To understand this result, one should refer to the theoretical results of the stability theory of a circular jet with finite boundary-layer thickness. It has been shown for this case (see Michalke 1971) that at low Strouhal numbers the boundary-layer thickness does not play an important role. The stability behaviour in this region can be determined by consideration of a circular jet with an infinitesimally thin boundary layer. It looks as if this conclusion can be extended to the case of a real jet issuing from a nozzle too.†

† This statement does not imply any consideration of the type of Kutta condition at the trailing edge of the nozzle.

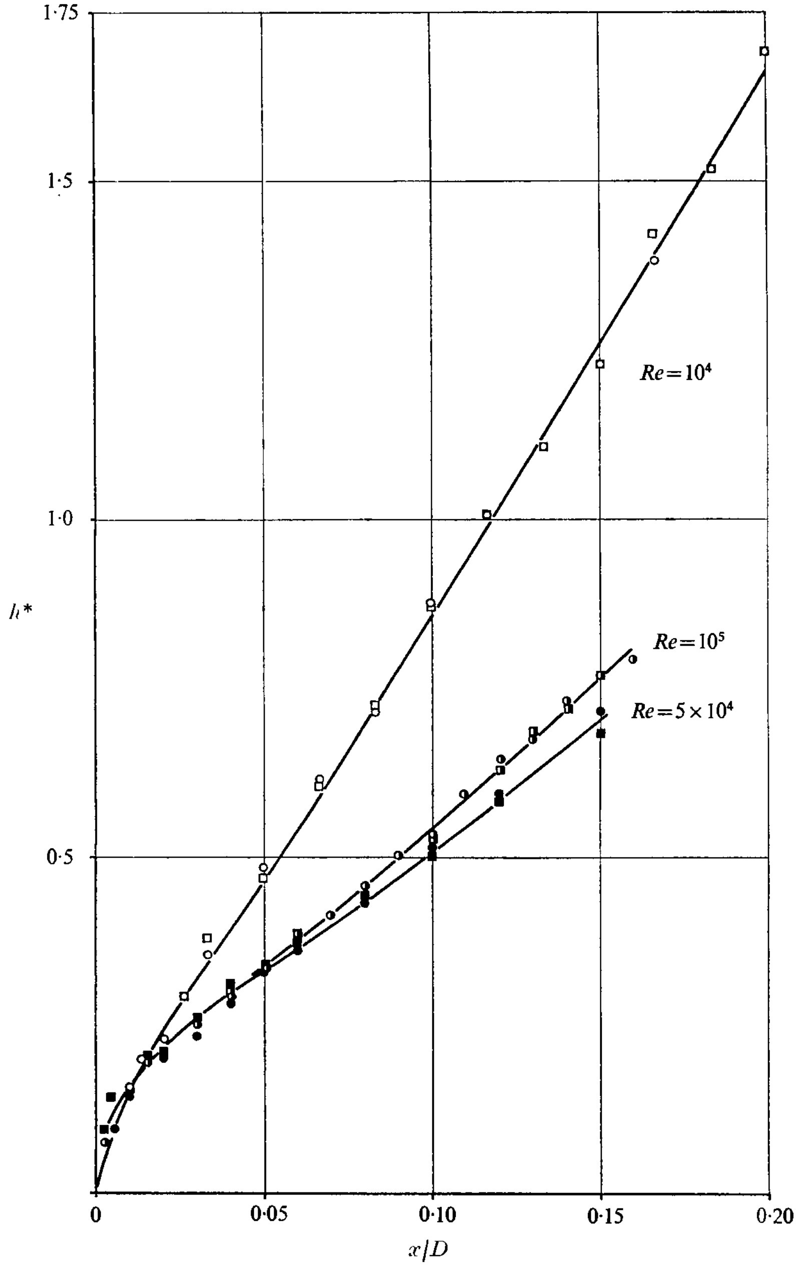

FIGURE 13. Optical compensation measurements: envelope of the jet border deflexion downstream. $S_D = 0{\cdot}725$. $Re = 10^4$: ○, 94 db; □, 84 db. $Re = 5 \times 10^4$: ●, 108 db; ■, 98 db. $Re = 10^5$: ◑, 118 db; ◨, 108 db.

At higher Strouhal numbers (figures 13 and 14) we see a divergence of the curves for the several Reynolds numbers. It turns out that the lowest Reynolds number corresponds to the highest amplification rate in the downstream direction. This observation can also be explained by reference to the theory of the

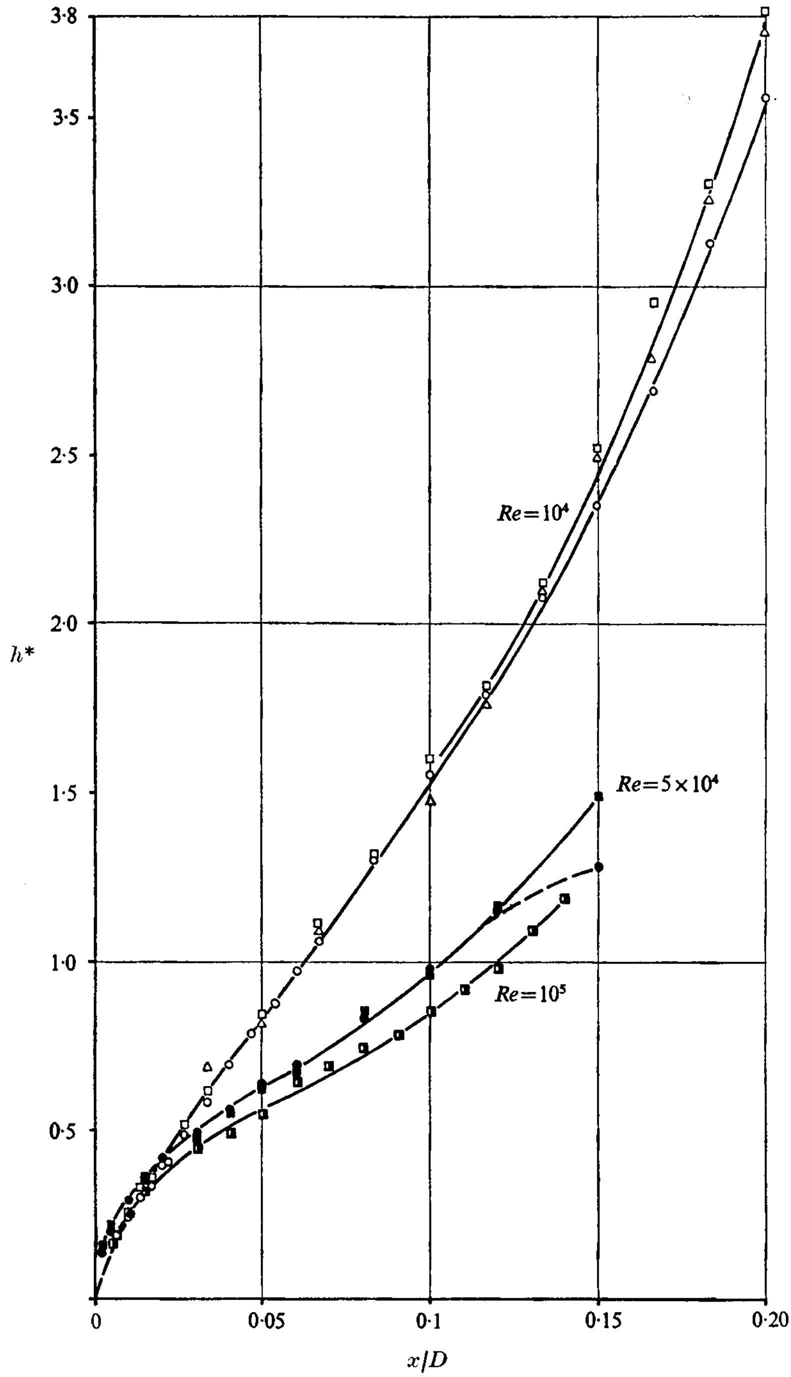

FIGURE 14. Optical compensation measurements: envelope of the jet border deflexion downstream. $S_D = 1{\cdot}015$. $Re = 10^4$: ○, 104 db; □, 94 db; △, 84 db. $Re = 5 \times 10^4$: ●, 108 db; ■, 98 db. $Re = 10^5$: ◨, 108 db.

infinitely long jet with finite boundary-layer thickness. If we consider the amplification rate of the stability waves in a circular jet, we find that at some low Strouhal number the amplification rate of the circular jet with finite boundar-layer thickness exceeds the amplification rate of the circular jet with an infinitesimally thin boundary layer. This effect occurs at lower Strouhal numbers for increasing boundary-layer thickness. An increasing boundary-layer thickness (i.e. R/θ becoming smaller) corresponds to a decreasing Reynolds number (equation (2)]. So we find that the divergence of the jet deflexion curves at higher Strouhal numbers has a simple explanation.

One might argue that in the problem under consideration the Strouhal number S_θ based on the boundary-layer thickness is a significant parameter. Nevertheless, we found no relation between the h^* curves at equal S_θ and at different Reynolds numbers. Obviously, it is not possible to collapse all measurements into a single curve, since the problem is (after having eliminated the compressibility effects), a real two-parameter one. For small Strouhal numbers only, the Reynolds number is not an important parameter. The Strouhal number region in which the Reynolds number does not play an important role becomes larger with decreasing boundary-layer thickness, i.e. with increasing Reynolds number in the case of a laminar flow.

In all our measurements of the jet border deflexion envelope h^*, we found a parabola-shaped region near the nozzle edge. The size of this region decreased with decreasing Strouhal number. The latter fact had not yet been discovered in a preceding paper of the authors (Bechert & Pfizenmaier 1971). The reason was that former measuring techniques have not had good enough measuring point resolution to detect this 'parabolic' region of the jet border deflexion. Nevertheless, the measured results of this previous work are not in question now. They have been verified to be in a surprisingly good agreement with the new optical compensation measurements (see Bechert & Pfizenmaier 1973).

The present experiments indicate that there is a gap between theory and experiment concerning the problem of the Kutta condition at the trailing edge of a nozzle (or even an airfoil). There are theories assuming an infinitesimally thin shear layer, while there are measurements with a real boundary layer which can hardly be interpreted by such theories. In spite of minor inconsistencies the following interpretation of the experiments seems to be reasonable.

Since one is most interested (for the purpose of understanding sound radiation) in the behaviour of the outer potential flow at the outer border of the shear layer, one wishes to obtain a simple description of *this* part of the problem. We expect a transition from the 'full Kutta condition' to the 'parabolic condition' with increasing Strouhal number. For a sufficiently low Strouhal number a description in terms of a linear superposition of both conditions is proposed. This might be understood by analogy with the result of Brown & Stewartson (1970), who obtained for the potential far field of an airfoil in a steady viscous flow a linear superposition of both conditions too.

If one tries a numerical comparison of the measured results with a 'mixed Kutta condition' composed of both explicit solutions of Orszag & Crow with coefficients adapted to the experiments, one obtains an excellent description of the magnitude of h^*. For $S_D > 1$ and $Re = 5 \times 10^4$ or 10^5 this comparison was made with the available data. We used a computer optimization procedure to fit the semi-empirical superposition approach to the experimental data. In all cases considered the deviations over the whole measuring range were smaller than the measurement accuracy. However, it is not possible to obtain *one* set of coefficients which produces reasonable agreement for all four measured quantities (h^*, ϕ_{RF}, $\tilde{u}_{\mathrm{r.m.s.}}$, ϕ_{HD}; see, for example, figure 8) at once. This is not astonishing because the theory of Orszag & Crow is based on boundary conditions quite different from those in our experiments. Moreover, especially at low Strouhal numbers (estimated at $S_D < 1$ from the theory of infinitely long jets), the axial symmetry plays an important role. Nevertheless, the authors feel that this 'mixed Kutta condition' concept should be mentioned here because it seems to incorporate most of the observed properties of the outer border of the shear layer in the vicinity of the trailing edge.

5. Conclusions

Deflexion measurements of the jet border in a weakly unsteady jet flow were performed. The measurements were focused on the region near the discharge edge of the nozzle. The location of the measurements was the dividing streamline between flow originating from the interior of the nozzle and the flow coming from outside.

The authors found the jet deflexion envelope to have a nearly parabolic shape near the nozzle edge. The size of this 'parabolic' region decreased with decreasing Strouhal number.

It was confirmed by the experiments that the unsteady motion in the vicinity of the trailing edge behaves linearly at low fluctuation amplitudes. Therefore no 'rectification effect' of the flow (i.e. a reaction of the mean flow caused by the alternating flow) takes place. Nonlinearities first occur in the region of saturation of the fluctuations in the free shear layer, somewhere downstream of the nozzle edge.

Since the behaviour of the exterior border of the jet contains information about the radiated sound field, a simple model for this part of the problem is proposed. To simulate the transition from the 'full Kutta condition' to the 'parabolic condition' with increasing Strouhal number, a linear combination of both contributions (obtained from Orszag & Crow's theoretical model) is introduced. The observed growth of the parabolic region of the jet envelope near the nozzle edge with increasing Strouhal number can be simulated by this model. Moreover, for the data considered, an excellent approximation to the jet envelope is obtained. Nevertheless, the Strouhal number range where theory and experiment can be compared is still too limited to be able to decide the general significance of this new semi-empirical model.

In connexion with the present work a new optical measuring technique has been developed, and enabled us to solve the measuring problems, related to the fluctuating flow near the nozzle discharge edge. The measuring resolution for the jet border deflexion measurements was of the order of 1–3 μm.

The idea for the new optical measuring technique resulted from some discussions with Professor H. Bossel from the University of Santa Monica, who stayed together with one of the authors (D. B.) as a visiting professor at the Max-Planck-Institut für Strömungsforschung in Göttingen. The experimental work was carried out at the DFVLR-Institut für Turbulenzforschung in Berlin, which was under the direction of the late Professor Dr.-Ing. Rudolf Wille. The authors would like to thank Dipl.-Ing. B. Lehmann for his help in constructing the optical apparatus. The laser equipment was borrowed from the Sonderforschungsbereich Magnetohydrodynamik of the Technische Universität Berlin. Through the kind help of the Institut für Technische Akustik (TU Berlin) it was possible to replace our own electronic equipment, which failed. The greater part of the measuring equipment, including the free jet test facility, was provided through financial support of the Deutsche Forschungsgemeinschaft.

REFERENCES

BECHERT, D. 1971 About some simplifications concerning calculations in aeroacoustics [in German]. *D.L.R. Rep.* FB 71–25.

BECHERT, D. & MICHEL, U. 1974 The control of a thin free shear layer with and without a semi-infinite plate with a pulsating monopole or dipole. Some new closed form solutions. *D.L.R. Rep.* FB 74–22.

BECHERT, D. & MICHEL, U. 1975 The control of a thin free shear layer with and without a semi-infinite plate by a pulsating flow field. *Acustica*, **33** (to appear).

BECHERT, D. & PFIZENMAIER, E. 1971 On the Kutta condition at the nozzle discharge edge in a weakly unsteady nozzle flow [in German]. *D.L.R. Rep.* FB 71–09. (Trans. *R.A.E. Lib. Trans.* no. 1617.)

BECHERT, D. & PFIZENMAIER, E. 1973 Optical compensation measurements on the unsteady exit condition at a nozzle discharge edge. An investigation in connection with sound transmission through nozzles with flow [in German]. *D.L.R. Rep.* FB 73–93.

BROWN, S. N. & STEWARTSON, K. 1970 Trailing-edge stall. *J. Fluid Mech.* **42**, 561.

CRIGHTON, D. G. 1972*a* Radiation properties of the semi-infinite vortex sheet. *Proc. Roy. Soc.* A **330**, 185.

CRIGHTON, D. G. 1972*b* The excess noise field of subsonic jets. *J. Fluid Mech.* **56**, 683.

CRIGHTON, D. G. & LEPPINGTON, F. G. 1974 Radiation properties of the semi-infinite vortex sheet: the initial-value problem. *J. Fluid Mech.* **64**, 393.

FREYMUTH, P. 1966 On transition in a separated laminar boundary layer. *J. Fluid Mech.* **25**, 683.

LIGHTHILL, M. J. 1952 On sound generated aerodynamically: I. *Proc. Roy. Soc.* A **211**, 564.

LIGHTHILL, M. J. 1954 On sound generated aerodynamically: II. *Proc. Roy. Soc.* A **222**, 1.

MICHALKE, A. 1962 Theoretical and experimental investigation of an axisymmetrical laminar boundary layer of a nozzle [in German]. *Ing. Arch.* **31**, 268.

MICHALKE, A. 1965 On spatially growing disturbances in an inviscid shear layer. *J. Fluid Mech.* **23**, 521.

MICHALKE, A. 1971 Instability of a compressible circular jet with reference to the influence of the free jet boundary layer thickness [in German]. *Z. Flugwiss.* **19**, 319.

MIKSAD, R. W. 1972 Experiments on the nonlinear stages of free-shear-layer transition. *J. Fluid Mech.* **56**, 695.

MÖHRING, W. 1975 On flows with vortex sheets and solid plates. *J. Sound Vib.* **38**, 403.

ORSZAG, S. A. & CROW, S. C. 1970 Instability of a vortex sheet, leaving a semi-infinite plate. *Studies of Appl. Math.* **49**, 167.

PFIZENMAIER, E. 1973 On the instability of the sound-influenced free jet [in German]. *D.L.R. Rep.* FB 73–69. (Trans. Esro TT–122.)

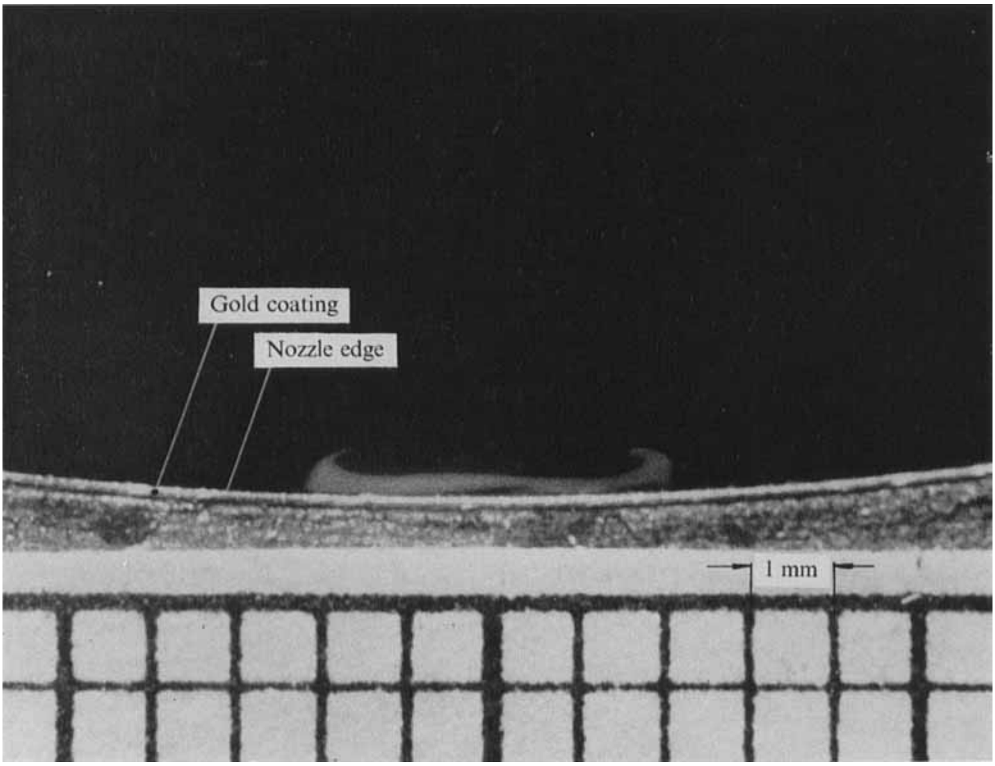

FIGURE 5. Cross-section of the smoke filament at $Re = 5 \times 10^4$; nozzle diameter = 100 mm.